

Reflected multi-entropy and its holographic dual

Ma-Ke Yuan,^{1,*} Mingyi Li,^{1,†} and Yang Zhou^{1,‡}

¹*Department of Physics and Center for Field Theory and Particle Physics, Fudan University, Shanghai 200433, China*

We introduce a mixed-state generalization of the multi-entropy through the canonical purification, which we call reflected multi-entropy. We propose the holographic dual of this measure. For the tripartite case, a field-theoretical calculation is performed using a six-point function of twist operators at large c limit. At both zero and finite temperature, the field-theoretical results match the holographic results, supporting our holographic conjecture of this new measure.

Introduction

Quantum entanglement [1, 2] has recently emerged as a key tool in understanding the AdS/CFT correspondence [3–5], which remains one of our most successful frameworks for probing quantum gravity. Remarkably, the Ryu-Takayanagi formula [6–9] provides a means to calculate entanglement entropy (EE) in conformal field theories (CFTs) via the minimal area of a codimension-2 surface in anti-de Sitter (AdS) space, establishing a precise link between spacetime geometry and quantum entanglement. However, EE exclusively captures quantum entanglement for pure states. To extend this connection to mixed states, holographic duals for several other measures, such as the entanglement of purification [10–12], reflected entropy [13–15], logarithmic negativity [16–20], and odd entanglement entropy [21, 22], have recently been studied. Another important direction lies in the investigation of multipartite correlation measures [23–30], whose holographic duals play a critical role in understanding the emergence of bulk spacetime from the boundary many-body quantum entanglement. The aim of this Letter is to bridge the gap between multipartite correlations in mixed states and spacetime geometry.

For a given multipartite mixed state, we can canonically purify it to obtain a pure state [13]. Using the recent proposal for pure state multipartite entanglement measure [31] based on the replica trick and permutation invariance, one can compute the so-called multi-entropy for the purified state. We propose this as an intrinsic multipartite measure for the original mixed state, which we term *reflected multi-entropy*. Unlike multi-entropy [32–35], reflected multi-entropy is intrinsically well-defined in the ultraviolet, thus circumventing the divergence issue that plagues EE as well as multi-entropy in quantum field theory. We note that while the multipartite generalizations of reflected entropy have been studied in [36, 37][38], these attempts are fundamentally distinct from our approach. Crucially, unlike these previous measures in [36, 37]—which are defined through the von Neumann entropy on replica spaces—our proposed reflected multi-entropy is fundamentally rooted in multi-entropy, an intrinsic multipartite entanglement measure.

In the remainder of this Letter, we first introduce reflected multi-entropy as the mixed-state generalization

of multi-entropy, and then propose its holographic dual. For the tripartite case, we perform a field-theoretical calculation using a six-point function of twist operators and find that it matches the holographic result, both at zero and finite temperature.

A Generalization of multi-entropy

Review of multi-entropy. Let us recall some basic notions of EE and Rényi entropy. Given a pure state $|\psi\rangle_{AB}$ that describes two systems A and B , the EE between them is defined as

$$S(A) = -\text{Tr}\rho_A \log \rho_A , \quad (1)$$

where $\rho_A = \text{Tr}_B |\psi\rangle \langle \psi|_{AB}$ is the reduced density matrix. Rényi entropy is a one-parameter generalization of EE

$$S_n(A) = \frac{1}{1-n} \log \text{Tr}\rho_A^n , \quad (2)$$

which reduces to EE (1) in the limit $n \rightarrow 1$. This is called *replica trick*. In order to introduce the multi-entropy, let us reformulate ρ_A^n through the permutation and contraction of the indices of the n copies of ρ_A ,

$$\begin{aligned} \rho_A^n &= (\rho_A)_{\alpha_1}^{\alpha_2} (\rho_A)_{\alpha_2}^{\alpha_3} (\rho_A)_{\alpha_3}^{\alpha_4} \cdots (\rho_A)_{\alpha_n}^{\alpha_1} \\ &= (\rho_A)_{\alpha_1}^{\alpha_{\sigma \cdot 1}} (\rho_A)_{\alpha_2}^{\alpha_{\sigma \cdot 2}} (\rho_A)_{\alpha_3}^{\alpha_{\sigma \cdot 3}} \cdots (\rho_A)_{\alpha_n}^{\alpha_{\sigma \cdot n}} , \end{aligned} \quad (3)$$

with $\sigma = (123 \cdots n)$ the permutation acting on the index of replicas. Guided by this key observation, in [31] the authors defined the *multi-entropy* $S^{(q)}$, which generalizes the concept of EE to q -partite cases through the permutation and contraction of indices. Let us focus on tripartite pure state $|\psi\rangle_{ABC}$ to illustrate.

Like Rényi entropy, the entanglement measure $S_n^{(q=3)}$ should be determined by the choice of permutation $(\sigma_A, \sigma_B, \sigma_C)$ acting on the replica indices, i.e., the way of contracting multiple density matrices. Note that there is a equivalence relation $(\sigma_A, \sigma_B, \sigma_C) \sim (\sigma_A, \sigma_B, \sigma_C) \cdot g$ allowing us to set $\sigma_A = \text{id}$ by choosing $g = \sigma_A^{-1}$, reducing the problem to $(q-1)$ -parties with the entanglement measure depending solely on (σ_B, σ_C) [41]. Both B and C have n replicas and (σ_B, σ_C) are chosen to be cyclic permutations of order n . In total, we have $n^{q-1} = n^2$

replicas, which form a $n \times n$ square lattice. The multi-entropy is defined by choosing the replica symmetry as $\mathbb{Z}_n \otimes \mathbb{Z}_n$ with the first or second \mathbb{Z}_n acting on the subregion B or C and cyclically permuting the replicas located in the same row or column of the lattice.

For general n and q -partite entanglement, the Rényi multi-entropy is defined as [31, 34] [42]

$$S_n^{(q)} = \frac{1}{1-n} \frac{1}{n^{q-2}} \log \left(\mathcal{Z}_{n^{q-1}}^{(q)} / (\mathcal{Z}_1^{(q)})^{n^{q-1}} \right), \quad (4)$$

where $\mathcal{Z}_{n^{q-1}}^{(q)}$ is the partition function on the n^{q-1} -sheet Riemann surface with replica symmetry $\mathbb{Z}_n^{\otimes (q-1)}$ as described above. The multi-entropy is defined by taking the $n \rightarrow 1$ limit,

$$S^{(q)} = \lim_{n \rightarrow 1} S_n^{(q)}. \quad (5)$$

For $q = 3$ and $n = 2$, the partition function contains four replicas with the gluing $\sigma_B = (13)(24)$ and $\sigma_C = (12)(34)$ as illustrated in Fig. 1 via the Euclidean path integral [43–45]. This results in a contraction of four

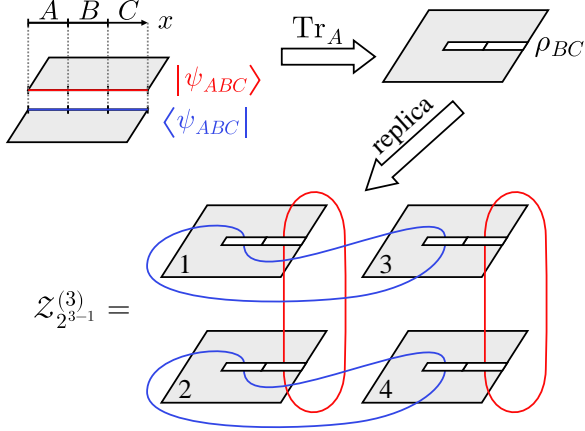


FIG. 1. The construction of the n^{q-1} -sheet Riemann surface in the special case $q = 3$ and $n = 2$.

density matrices (here we abbreviate ρ_{BC} as ρ),

$$\mathcal{Z}_{2^{3-1}}^{(3)} = \rho_{\beta_1 \chi_1}^{\beta_3 \chi_2} \rho_{\beta_2 \chi_2}^{\beta_4 \chi_1} \rho_{\beta_3 \chi_3}^{\beta_1 \chi_4} \rho_{\beta_4 \chi_4}^{\beta_2 \chi_3}. \quad (6)$$

The corresponding Rényi multi-entropy is then given by (4) with $\mathcal{Z}_1^{(3)} = \rho_{\beta_X}^{\beta_X}$ serving as the normalization factor.

Mixed-state generalization of multi-entropy through canonical purification. A multipartite mixed state can be obtained by tracing out some part from a pure state. Again we will focus on tripartite case with $q = 3$ but it can be generalized to larger q straightforwardly. Starting from a pure state $\psi_{AcBaCb} \in \mathcal{H}_{AcBaCb}$ and tracing out abc , we obtain a mixed state ρ_{ABC} , which can be canonically purified by doubling the Hilbert space (see Fig. 2 for a schematic diagram of this purification process). For more discussions on canonical purification we

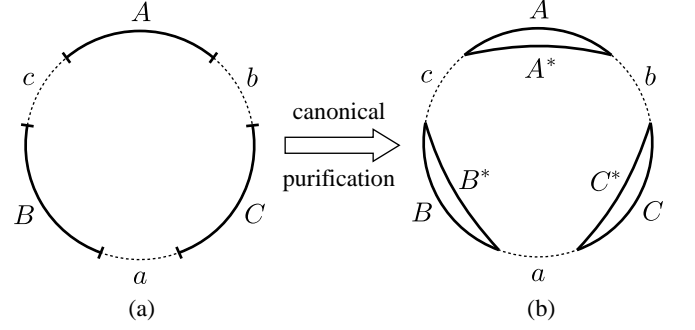


FIG. 2. Canonical purification of ρ_{ABC} . (a) Global pure state ψ_{AcBaCb} defined on a circle. Tracing out abc gives a mixed state ρ_{ABC} . (b) Picking up another copy of ρ_{ABC} and gluing these two copies along abc gives a big pure state $|\sqrt{\rho_{ABC}}\rangle$ (7), which is the canonical purification of ρ_{ABC} .

refer to [13]. The purified state can be expressed as

$$\begin{aligned} |\sqrt{\rho_{ABC}}\rangle &= |\sqrt{\text{Tr}_{abc} |\psi_{AcBaCb}\rangle \langle \psi_{AcBaCb}|}\rangle \\ &\in (\mathcal{H}_A \otimes \mathcal{H}_A^*) \otimes (\mathcal{H}_B \otimes \mathcal{H}_B^*) \otimes (\mathcal{H}_C \otimes \mathcal{H}_C^*). \end{aligned} \quad (7)$$

We define the *reflected multi-entropy* as

$$S_R^{(q=3)}(A; B; C) = S^{(q=3)}(AA^*; BB^*; CC^*)_{|\sqrt{\rho_{ABC}}\rangle}, \quad (8)$$

with $S^{(q)}$ the original multi-entropy (5). The subscript R in $S_R^{(q)}$ denotes “reflected” [46].

Here we list some properties of reflected multi-entropy,

- (A) It reduces to twice the multi-entropy for pure state $\rho_{AB\dots} = |\psi\rangle \langle \psi|_{AB\dots}$,
pure state: $S_R^{(q)}(A; B; \dots) = 2S^{(q)}(A; B; \dots)$. (9)
- (B) It reduces to the reflected entropy [13] for bipartite system ρ_{AB} , i.e., $S_R^{(q=2)}(A; B) = S_R(A; B)$.
- (C) It vanishes for factorized density matrix $\rho_{AB\dots} = \rho_A \otimes \rho_B \otimes \dots$,
product state: $S_R^{(q)}(A; B; \dots) = 0$. (10)

However, $S_R^{(q)}(A; B; \dots)$ can be nonzero for separable states. Consider a simple separable state:

$$\rho_{ABC} = \frac{1}{2} |000\rangle \langle 000| + \frac{1}{2} |111\rangle \langle 111|. \quad (11)$$

Its canonical purification is a GHZ state $\frac{1}{2} |000000\rangle + \frac{1}{2} |111111\rangle$ with nonzero $S_R^{(3)}(A; B; C) = \frac{3}{2} \log 2$.

- (D) It is bounded from below by multi-entropy of purification,

$$\text{lower bound: } S_R^{(q)}(A; B; \dots) \geq M_P(A; B; \dots), \quad (12)$$

where the multi-entropy of purification M_P is defined by minimization of multi-entropy over all possible purifications.

(E) It is bounded from below by half the multipartite reflected entropy [37] for holographic states,

$$\text{lower bound: } S_R^{(q)}(A; B; \dots) \geq \frac{1}{2} \Delta_R(A; B; \dots) . \quad (13)$$

Holography of reflected multi-entropy

Based on the canonical purification for holographic states [13] and the holographic proposal for multi-entropy [31], now we want to find the holographic dual for reflected multi-entropy. Consider a global pure state ψ_{AcBaCb} defined on a circle as shown in Fig. 2(a). This pure state has a classical bulk solution as its holographic dual. Now we trace out abc , which corresponds to retaining only the entanglement wedge for ρ_{ABC} and pre-scinding the other portion of the bulk. To perform the canonical purification, we pick up another copy of the entanglement wedge and glue these two copies along the Ryu-Takayanagi surface (RT surface) for ρ_{ABC} . The resulting geometry is drawn in Fig. 3(a).

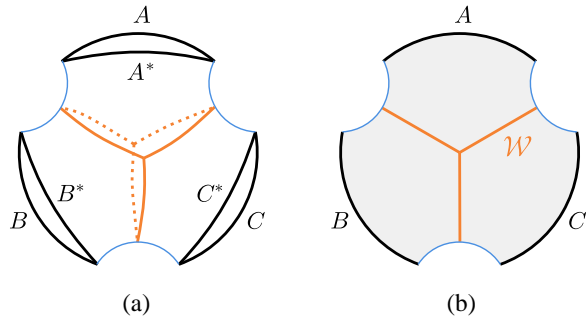


FIG. 3. (a) Canonical purification of ρ_{ABC} and its holographic dual. Tracing out abc corresponds to gluing along the RT surface for ρ_{ABC} (blue curves). The orange web \mathcal{W} is the minimal web in the bulk as the holographic dual of $S^{(3)}(AA^*; BB^*; CC^*)$. (b) The single copy picture. The shadow area is the entanglement wedge of $A \cup B \cup C$ and the orange web is the holographic dual of $S_R^{(3)}(A; B; C)$.

To figure out the geometry dual of the reflected multi-entropy, which now becomes the multi-entropy between AA^* , BB^* , and CC^* , we need to generalize the holographic proposal for multi-entropy [31] to multi-boundary pure states. Recall that the original holographic proposal for multi-entropy is a minimal bulk web \mathcal{W} consisting of minimal codimension-2 surfaces. For a single boundary pure state, \mathcal{W} is anchored at the boundaries of all subsystems A, B, \dots . This condition is relaxed in the case of multi-boundary, much like the RT surfaces for multi-boundary states. Another important condition is that \mathcal{W} should contain subwebs that are homologous to all the subsystems A, B, \dots . This can be easily satisfied. It is then natural to propose the holographic dual of the reflected multi-entropy as the minimal surface web

shown in Fig. 3(a). More precisely, the holographic dual of the reflected multi-entropy $S_R^{(q)}(A; B; \dots)$ is the minimal surface web \mathcal{W} satisfying the following topological conditions:

- (1) \mathcal{W} is anchored at the RT surface for $A \cup B \cup \dots$.
- (2) \mathcal{W} contains subwebs that are homologous to all the subsystems A, B, \dots .

The holographic reflected multi-entropy is computed by

$$S_R^{(q)} = \frac{2}{4G_N} \min_{\mathcal{W}} L[\mathcal{W}] , \quad (14)$$

with $L[\mathcal{W}]$ the area of the web \mathcal{W} in a single copy as illustrated in Fig. 3(b).

Computation in $\text{AdS}_3/\text{CFT}_2$

Let us study a simple example in $\text{AdS}_3/\text{CFT}_2$, as illustrated in Fig. 4. We work in Poincaré half plane with the metric

$$ds^2 = \frac{dx^2 + dy^2}{y^2} , \quad x \in \mathbb{R} \text{ & } y \in \mathbb{R}_+ . \quad (15)$$

We consider the reflected multi-entropy $S_R^{(3)}(A; B; C)$ between subsystems A, B, C . ρ_{ABC} is a mixed state obtained by tracing out abc from the pure state ψ_{AcBaCb} defined on \mathbb{R} as shown in Fig. 4. The subsystems A, B, C are chosen to be $A = [x_1, x_2]$, $B = [x_3, x_4]$, $C = [x_5, x_6]$ with $x_{i=1, \dots, 6}$ parametrized by $\xi = a, b, c$,

$$\begin{aligned} x_6 &= -x_1 = b , \\ x_5 &= -x_2 = a + r , \quad x_4 = -x_3 = a - r . \end{aligned} \quad (16)$$

In the following we will calculate $S_R^{(3)}(A; B; C)$ using both holographic method and field-theoretical method and find the agreement between them.

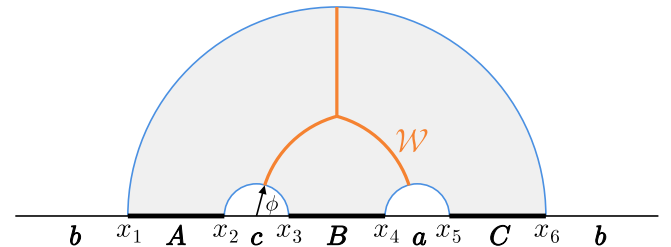


FIG. 4. The holographic dual of $S_R^{(q=3)}(A; B; C)$.

Holographic calculation. The holographic dual of $S_R^{(3)}(A; B; C)$ is the minimal web denoted by the orange curves in Fig. 4. Because of the \mathbb{Z}_2 -symmetry about the $x = 0$ axis in Fig. 4, the junction I is expected to be on $x = 0$ and we denote it by $I(0, y_I)$. For general two

points (x_1, y_1) and (x_2, y_2) on the Poincaré half plane, the distance between them is

$$D((x_1, z_1), (y_2, y_2)) = \operatorname{arccosh} \frac{(x_1 - x_2)^2 + y_1^2 + y_2^2}{2y_1 y_2}. \quad (17)$$

Therefore, the distance between I and the RT surface of c is given by

$$\min_{\phi} D((0, y_I), (-a + r \cos \phi, r \sin \phi)), \quad (18)$$

with $(-a + r \cos \phi, r \sin \phi)$ a point on the RT surface of c . The distances between I and the RT surface of a, b can be worked out similarly and we finally end up with the length of the bulk dual web

$$L[\mathcal{W}](a, b, r) = \min_{y_I} \left[\log(b/y_I) + 2 \operatorname{arcsech} \frac{2y_I r}{\sqrt{((a - r)^2 + y_I^2)((a + r)^2 + y_I^2)}} \right], \quad (19)$$

where the first and second term in $[\dots]$ comes from the distance between I and the RT surface of b and $\{a, c\}$. The minimization over y_I in (19) will be evaluated numerically (see the blue curves in Fig. 5) when comparing with the field-theoretical results.

Field-theoretical calculation. Now we do the calculation in CFT_2 . Using the replica trick, we first represent the reflected multi-entropy as a path integral on a specific Riemann surface. Here, a new replica number m is introduced for canonical purification (see Ref. [13] for more details about this replica trick).

The n -th Rényi version of reflected multi-entropy is

$$S_R^{(q)}[n] = \frac{1}{1-n} \frac{1}{n^{q-2}} \log \frac{\mathcal{Z}_{n^{q-1},m}}{(\mathcal{Z}_{1,m})^{n^{q-1}}}, \quad (20)$$

and the reflected multi-entropy is obtained by taking the limit $n \rightarrow 1$ and $m \rightarrow 1$,

$$S_R^{(q)} = \lim_{m \rightarrow 1} \lim_{n \rightarrow 1} \frac{1}{1-n} \frac{1}{n^{q-2}} \log \frac{\mathcal{Z}_{n^{q-1},m}}{(\mathcal{Z}_{1,m})^{n^{q-1}}}. \quad (21)$$

Now we use the twist operator correlation function to express $\mathcal{Z}_{n^{q-1},m}$, the path integral on a glued Euclidean spacetime with mn^{q-1} copies. The conformal weights h_i of twist operators $\sigma_i(x_i)$ can be read from the representation of cyclic groups [47],

$$h_{i=1, \dots, 2q} = \frac{c}{24} \left(m - \frac{1}{m} \right) n^{q-1}. \quad (22)$$

We leave the derivation of the conformal weights (22) and (23) to Supplemental Material [48]. When $q = 2$, one can check that (22) reduces to the conformal weight of the twist operators for the reflected entropy as we expected [49]. The conformal weights h_a of the leading operators σ_a in operator product expansion $\sigma_i(x_i)\sigma_j(x_j) \rightarrow \sigma_{a=ij}(x_a)$ are

$$h_{a=ij} = \frac{c}{12} (n^{q-1} - n^{q-3}), \quad (23)$$

which is twice the conformal weight of the twist operators for the original multi-entropy as we expected [50]. It can also be checked that for $q = 2$, (23) reduces to twice the conformal weight of the twist operators for EE.

Using these twist operators, $\mathcal{Z}_{n^{q-1},m}$ can be represented by the six-point function

$$\mathcal{Z}_{n^{q-1},m} = \langle \sigma_1 \sigma_2 \sigma_3 \sigma_4 \sigma_5 \sigma_6 \rangle_{\text{CFT}^{\otimes mn^{q-1}}}, \quad (24)$$

with σ_i located at x_i . At large c limit, the calculation of (24) can be converted to solving a monodromy problem [51, 52]. Following the approach in [53] we compute the six-point function (24) at large c limit [48] and the partial derivatives of $S_R^{(3)}(A; B; C)$ with respect to a, b, r are plotted in Fig. 5.

On the other hand, the holographic result is given by minimizing $L[\mathcal{W}](a, b, r)$ in (19). The partial derivatives of $(c/3)L[\mathcal{W}](a, b, r)$ with respect to a, b, r are plotted in Fig. 5 and compared with the field-theoretical results. These two results match precisely. Notice that we are comparing the derivatives of the entropy. To match the entropy itself, we have to further include the contributions of the operator product expansion coefficients in the CFT calculation [48].

We also examine the agreement between the field-theoretical and holographic results at finite temperature. From the CFT perspective, we compute the six-point function on an infinitely long cylinder with period β_{CFT} while on the gravity side, the bulk dual web length is evaluated in the Bañados-Teitelboim-Zanelli (BTZ) black hole background [54] [48]. We find that the reflected multi-entropy decreases with increasing temperature, indicating that thermal effects tend to wash out multipartite correlations. In the context of thermal systems, our proposal provides a concrete multipartite measure, whose potential connections to quantum chaos and information scrambling warrant further investigation. Another promising application of reflected multi-entropy is to explore whether it can serve as a diagnostic of topological order in mixed states [55, 56].

Discussion

In this Letter we introduced reflected multi-entropy as a multipartite measure for mixed state by combining the recent proposal of multi-entropy and canonical purification and found good agreement between the CFT results and the holographic results. One may worry about the potential bulk replica symmetry breaking for multi-entropy. While the bulk replica symmetry was assumed in the original holographic derivation [31, 32], recent work [27] shows this fails for $n > 2$ [57]. A similar issue arises for reflected multi-entropy with $n > 2$. Nevertheless, our holographic calculation focuses on the $n = 1$ case, evading the replica symmetry-breaking regime and

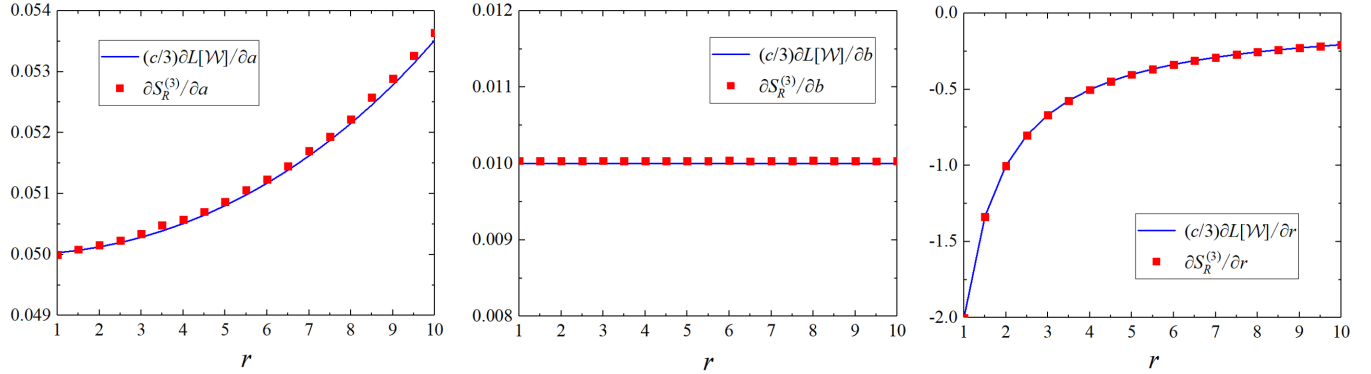


FIG. 5. Comparison of the partial derivatives of $\frac{c}{3}L[\mathcal{W}]$ and $S_R^{(q=3)}$ (divided by $c/3$) with respect to $\xi = a, b, r$ at zero temperature. We take $a = 20$, $b = 100$, and r ranging from 1 to 10. The holographic results and the field-theoretical results match well (the difference between them is within 0.4%).

ensuring the validity of our results. Our findings strongly support a new class of duality between multipartite measures for mixed states and spacetime geometry. Moreover, there are two natural extensions of our work. First, our discussion can be generalized straightforward to multiple canonical purifications. Second, similar to the covariant generalizations of reflected entropy and multi-entropy [13, 31], we expect that the ‘‘covariant reflected multi-entropy’’ is obtained as the area of the minimal extremal surface web rather than the global minimal one.

Note added. Recently, the authors in [59] found a special quantum state where the reflected entropy is not monotonically decreasing under partial trace thus fails to be a correlation measure. However, the reflected entropy remains a valid correlation measure for holographic states, as emphasized in the same paper. See also Ref. [60] for the monotonicity property of reflected entropy in free fields.

Acknowledgements. We are grateful for useful discussions with our group members in Fudan University. We would like to thank Jinwei Chu for helpful discussions. This work is supported by NSFC grant 12375063. This work is also sponsored by Natural Science Foundation of Shanghai (21ZR1409800) as well as Shanghai Talent Development Fund.

SUPPLEMENTAL MATERIAL

Derivation of conformal weights

In this section we derive the conformal weights of $\sigma_{i=1,\dots,2q}$ and $\sigma_{a=ij}$

$$h_{i=1,\dots,2q} = \frac{c}{24} \left(m - \frac{1}{m} \right) n^{q-1}, \quad (25)$$

$$h_{a=ij} = \frac{c}{12} (n^{q-1} - n^{q-3}) \quad (26)$$

from the path integral representation of $\mathcal{Z}_{n^{q-1},m}$. We consider the $\{q = 3, n = 3, m = 2\}$ case as an example. Replica trick in Fig. 7 is determined by six twist operators $\sigma_{i=1,\dots,6}$ located at the endpoints of the subsystems A, B, C (see top left corner of Fig. 6).

These twist operators are made up of three nontrivial operators $\Sigma_{A,B,C}$ associated with the three subsystems A, B, C respectively, which can be described by representation of cyclic groups. For instance, (123) in Σ_A means that the lower edge of subsystem A in the 1st copy is glued to the upper edge of A in the 2nd copy, the lower edge of A in the 2nd copy is glued to the upper edge of A in the 3rd copy, and the lower edge of A in the 3rd copy is glued to the upper edge of A in the 1st copy.

From Fig. 7 we can read

$$\begin{aligned} \Sigma_A &= (1, 2)(3, 4)(5, 6)(7, 8)(9, 10)(11, 12)(13, 14)(15, 16)(17, 18); \\ \Sigma_B &= (2, 7)(8, 13)(14, 1)(4, 9)(10, 15)(16, 3)(6, 11)(12, 17)(18, 5); \\ \Sigma_C &= (2, 3)(4, 5)(6, 1)(8, 9)(10, 11)(12, 7)(14, 15)(16, 17)(18, 13). \end{aligned} \quad (27)$$

Then we have

$$\sigma_1 = \Sigma_A, \quad \sigma_2 = \Sigma_A^{-1}, \quad \sigma_3 = \Sigma_B, \quad \sigma_4 = \Sigma_B^{-1}, \quad \sigma_5 = \Sigma_C, \quad \sigma_6 = \Sigma_C^{-1}. \quad (28)$$

Therefore, the conformal weights of σ_i [61] is $h_i = (c/24)(2 - 1/2) \times 9$, which is consistent with (25). For general $\{q, n, m\}$, since there are only m -cycles in $\sigma_{i=1,\dots,2q}$, their conformal weights h_i is thus given by (25).

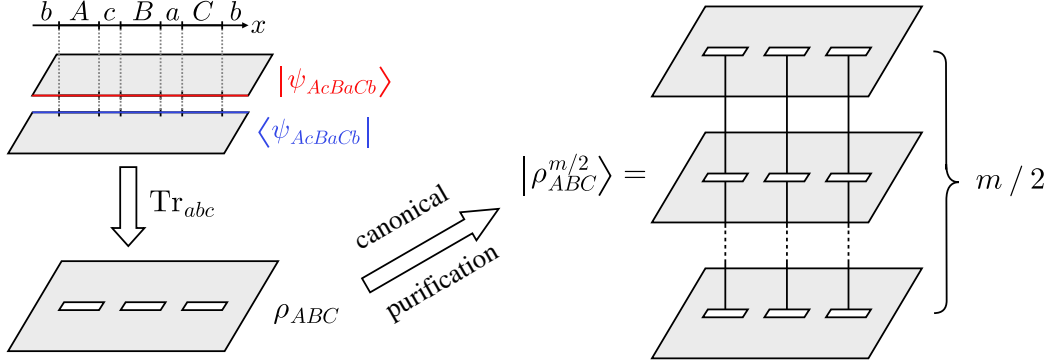


FIG. 6. Left: The path integral representation of the reduced density matrix ρ_{ABC} . Right: The path integral representation of $|\rho_{ABC}^{m/2}\rangle$, which is obtained from the canonical purification of ρ_{ABC} . Here m should be even and it will be analytically continued to 1 in the end.

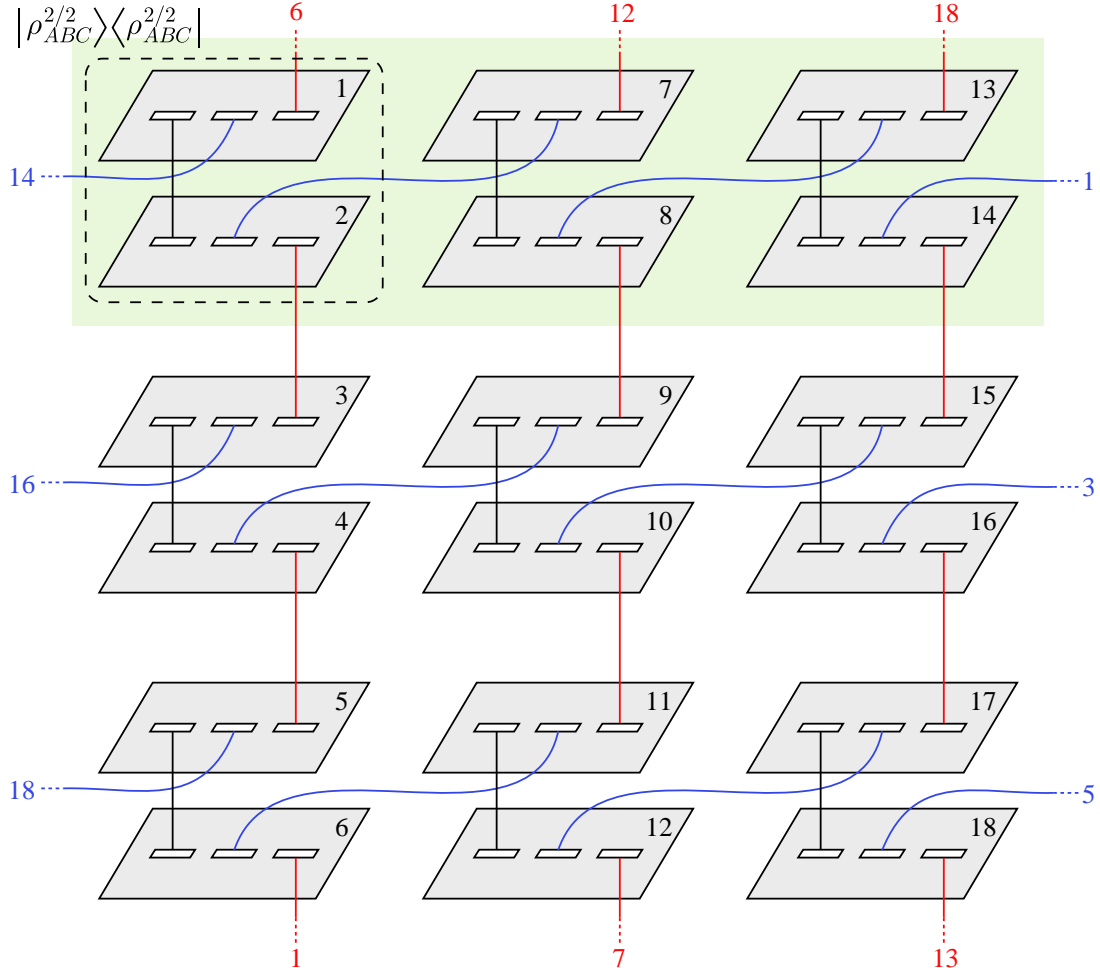


FIG. 7. The path integral representation of $\mathcal{Z}_{nq-1,m}$. Here we take $q = 3$, $n = 3$ and $m = 2$. The part inside the dashed box is the density matrix $|\rho_{ABC}^{2/2}\rangle \langle \rho_{ABC}^{2/2}|$. Some gluings involving replicas have not been shown. In this figure, if the lower edge of a subsystem in the i -th copy is glued to the upper edge in the j -th copy, then the upper edge of the same subsystem in the i -th copy is also glued to the lower edge in the j -th copy.

From (27) and (28), we can obtain leading operator $\sigma_{a=16,23,45}$ in the OPE of σ_i and σ_j

$$\begin{aligned}\sigma_{16} &= \sigma_1\sigma_6 = \Sigma_A \Sigma_C^{-1} = (1, 5, 3)(2, 4, 6)(7, 11, 9)(8, 10, 12)(13, 17, 15)(14, 16, 18) ; \\ \sigma_{23} &= \sigma_2\sigma_3 = \Sigma_A^{-1} \Sigma_B = (1, 13, 7)(2, 8, 14)(3, 15, 9)(4, 10, 16)(5, 17, 11)(6, 12, 18) ; \\ \sigma_{45} &= \sigma_4\sigma_5 = \Sigma_B^{-1} \Sigma_C = (1, 11, 15)(2, 16, 12)(3, 7, 17)(4, 18, 8)(5, 9, 13)(6, 14, 10) .\end{aligned}\quad (29)$$

Therefore, the conformal weights of σ_a are $h_a = (c/24)(3 - 1/3) \times 6$, which are consistent with (26). Now we generalize this result to general $\{q, n, m\}$ case, where we have mn^{q-1} copies and they form a $\underbrace{n \times n \times \cdots \times n}_{q-1}$ lattice with m copies

at each cell. We focus on the row containing the first cell [62] and consider the product of the parts of Σ_A^{-1} and Σ_B restricted to the cells in this row. We use $\tilde{\Sigma}_A$ and $\tilde{\Sigma}_B$ to denote the parts of Σ_A and Σ_B restricted to this row, and they are given by (since m is even, here we take $m = 2\ell$)

$$\begin{aligned}\tilde{\Sigma}_A &= (1, 2, \dots, \ell, \textcolor{red}{\ell+1}, \textcolor{red}{\ell+2}, \dots, \textcolor{red}{2\ell})(\textcolor{blue}{nm+1}, \textcolor{blue}{nm+2}, \dots, \textcolor{blue}{nm+\ell}, nm + \ell + 1, nm + \ell + 2, \dots, nm + 2\ell) \\ &\quad (2nm + 1, \dots, 2nm + 2\ell) \cdots ((n-1)nm + 1, \dots, (n-1)nm + 2\ell) , \\ \tilde{\Sigma}_B &= (\textcolor{red}{\ell+1}, \textcolor{red}{\ell+2}, \dots, \textcolor{red}{2\ell}, \textcolor{blue}{nm+1}, \textcolor{blue}{nm+2}, \dots, \textcolor{blue}{nm+\ell})(nm + \ell + 1, \dots, nm + 2\ell, 2nm + 1, \dots, 2nm + \ell) \cdots \quad (30) \\ &\quad ((n-2)nm + \ell + 1, \dots, (n-2)nm + 2\ell, (n-1)nm + 1, \dots, (n-1)nm + \ell) \\ &\quad ((n-1)nm + \ell + 1, \dots, (n-1)nm + 2\ell, 1, \dots, \ell) .\end{aligned}$$

The product $\tilde{\Sigma}_A^{-1} \tilde{\Sigma}_B$ is

$$\tilde{\Sigma}_A^{-1} \tilde{\Sigma}_B = (\ell, (n-1)nm + \ell, (n-2)nm + \ell, \dots, nm + \ell) (2\ell, nm + 2\ell, 2nm + 2\ell, \dots, (n-1)nm + 2\ell) , \quad (31)$$

which contains two n -cycles. One can check that when $n = 3, m = 2$, (30) and (31) reduces to (part of) (27) and (29). Note that our analysis here is restricted to a single row. Since there are n^{q-2} rows in total, the complete $\Sigma_A^{-1} \Sigma_B$ operator consists of $2n^{q-2}$ n -cycles, resulting in the conformal weight (26).

CFT computation of the six-point function

The reflected multi-entropy can be calculated by replica trick

$$S_R^{(q)} = \lim_{m \rightarrow 1} \lim_{n \rightarrow 1} \frac{1}{1-n} \frac{1}{n^{q-2}} \log \frac{\mathcal{Z}_{n^{q-1}, m}}{(\mathcal{Z}_{1, m})^{n^{q-1}}} , \quad (32)$$

with $\mathcal{Z}_{n^{q-1}, m}$ the partition function on a glued Euclidean spacetime with mn^{q-1} copies, which can be expressed using the twist operator correlation function. For the $q = 3$ case we are considering, it is given by a six-point function

$$\mathcal{Z}_{n^{3-1}, m} = \langle \sigma_1 \sigma_2 \sigma_3 \sigma_4 \sigma_5 \sigma_6 \rangle_{\text{CFT} \otimes mn^{3-1}} , \quad (33)$$

with the six points located at x_i

$$\begin{aligned}x_6 &= -x_1 = b , \\ x_5 &= -x_2 = a + r , \\ x_4 &= -x_3 = a - r\end{aligned}\quad (34)$$

and the relevant conformal weights given by (25) and (26). In this section we give a numerical calculation of

the six-point function (33). Utilizing the conformal transformation

$$x_i \rightarrow z_i = \frac{(x_i - x_2)(x_1 - x_6)}{(x_2 - x_6)(x_i - x_1)} , \quad (35)$$

$\{x_1, x_2, x_6\}$ are mapped to $\{z_1, z_2, z_6\} = \{\infty, 0, 1\}$ while $\{x_3, x_4, x_5\}$ are sent to $\{z_3, z_4, z_5\}$. At the large c limit with $h_{i=1, \dots, 6}/c$ and $h_{a=16, 23, 45}/c$ fixed (here h_i denotes the conformal weight of the external operator $\sigma_i(x_i)$ and h_a the weight of the internal operator), the six point function

$$\langle \sigma_1(z_1) \sigma_2(z_2) \sigma_3(z_3) \sigma_4(z_4) \sigma_5(z_5) \sigma_6(z_6) \rangle \quad (36)$$

can be approximated by

$$\begin{aligned}&\langle \sigma_1(z_1) \sigma_2(z_2) \sigma_3(z_3) \sigma_4(z_4) \sigma_5(z_5) \sigma_6(z_6) \rangle \\ &\approx c_{1,6}^{16} c_{2,3}^{23} c_{4,5}^{45} c_{16,23}^{45} \mathcal{F}(z_i) \mathcal{F}(\bar{z}_i) ,\end{aligned}\quad (37)$$

where $a = 16, 23, 45$ labels the leading order primary with conformal weight (26), $c_{i,j}^a$ is the OPE coefficient, and \mathcal{F} is the six-point Virasoro block, which exponentiates at large c limit [53]

$$\mathcal{F} \sim \exp \left[-\frac{c}{6} f \left(\frac{h_a}{c}, \frac{h_i}{c}, z_i \right) \right] . \quad (38)$$

Here f is called the semi-classical block, which can be obtained by solving the following monodromy problem. Consider the second-order differential equation

$$\psi''(z) + T(z) \psi(z) = 0 , \quad (39)$$

where $T(z)$ is given by

$$T(z) = \sum_{i=1}^6 \left(\frac{6h_i/c}{(z-z_i)^2} - \frac{c_i}{z-z_i} \right) , \quad (40)$$

with c_i the accessory parameters satisfying

$$\begin{aligned} \sum_{i=1}^6 c_i &= 0 , \\ \sum_{i=1}^6 (c_i z_i - 6h_i/c) &= 0 , \\ \sum_{i=1}^6 (c_i z_i^2 - 12z_i h_i/c) &= 0 , \end{aligned} \quad (41)$$

which guarantee that $T(z)$ vanishes as z^{-4} at infinity. As a second-order differential equation, (39) has two solutions ψ_1 and ψ_2 . Taking these solutions on a closed contour around some singular point, they will undergo some monodromy

$$\begin{pmatrix} \psi_1 \\ \psi_2 \end{pmatrix} \rightarrow M \begin{pmatrix} \psi_1 \\ \psi_2 \end{pmatrix} . \quad (42)$$

The accessory parameters c_i can be determined by (41) and the following three equations

$$\text{Tr} M_a = -2 \cos \left(\pi \sqrt{1 - \frac{24}{c} h_a} \right) , \quad a = 16, 23, 45, \quad (43)$$

where $M_{a=16}$ denotes the 2×2 monodromy matrix for the cycle γ_{16} enclosing z_1 and z_6 , and similarly for $a = 23, 45$; h_{16} is the conformal weight of the leading operator in

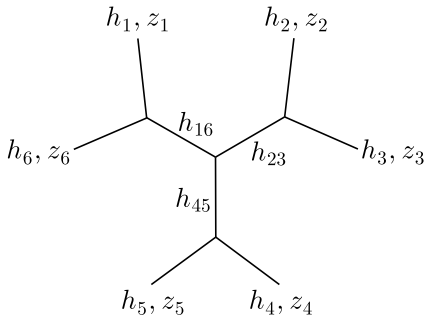


FIG. 8. Dominant fusion channel of the 6-point function (36).

the OPE contraction of $\sigma_1(z_1)$ and $\sigma_6(z_6)$ as shown in Fig. 8, similarly for $a = 23, 45$. From (26) we know that $h_{16} = h_{23} = h_{45} = \frac{c}{12}(n^2 - 1)$.

The relation between the semi-classical block f and the accessory parameters c_i is given by

$$\partial f / \partial z_i = c_i . \quad (44)$$

Therefore, we can calculate the partial derivative of $S_R^{(q)}$ with respect to the coordinate parameters $\xi = a, b, r$ in

(34). From (32), (33) and (37) we obtain

$$\begin{aligned} \frac{\partial S_R^{(q)}}{\partial \xi} &= \lim_{n \rightarrow 1} \frac{1}{n-1} \frac{1}{n^{3-2}} \frac{c}{3} \sum_{i=1}^6 \frac{\partial f}{\partial z_i} \frac{\partial z_i}{\partial \xi} \\ &= \lim_{n \rightarrow 1} \frac{1}{n-1} \frac{1}{n^{3-2}} \frac{c}{3} \sum_{i=1}^6 c_i \frac{\partial z_i}{\partial \xi} . \end{aligned} \quad (45)$$

Reflected multi-entropy at finite temperature

In this section we consider reflected multi-entropy in CFT at finite temperature, the bulk dual of which is the BTZ black hole [54]

$$ds^2 = \frac{1}{y^2} \left(f(y) d\tau^2 + \frac{dy^2}{f(y)} + dx^2 \right) , \quad (46)$$

where $f(y) = 1 - (y/y_H)^2$ with $y = y_H$ the horizon as shown in Fig. 9, $\tau \sim \tau + 2\pi y_H$, $\beta_{\text{CFT}} = 2\pi y_H$, and we have set the AdS radius to be 1. To be specific, we consider the reflected multi-entropy among the following three intervals

$$A = [-b, -a] , \quad B = [-a, a] , \quad C = [a, b] , \quad (47)$$

on the time slice $\tau = 0$ as illustrated in Fig. 9. To simplify, we consider the case that b goes to infinity.

Holographic calculation.

Now we compute the holographic reflected multi-entropy in the presence of BTZ black hole. The distance between two arbitrary points (τ, x, y) and (τ', x', y') in the BTZ metric (46) is given by

$$\begin{aligned} \tilde{D}((\tau, x, y), (\tau', x', y')) \\ = \text{arccosh} (T_1 T_1' + T_2 T_2' - X_1 X_1' - X_2 X_2') , \end{aligned} \quad (48)$$

with

$$\begin{aligned} T_1 &= \sqrt{\frac{y_H^2}{y^2} - 1} \sinh \frac{\tau}{y_H} , \quad T_2 = \frac{y_H}{y} \cosh \frac{x}{y_H} , \\ X_1 &= \sqrt{\frac{y_H^2}{y^2} - 1} \cosh \frac{\tau}{y_H} , \quad X_2 = \frac{y_H}{y} \sinh \frac{x}{y_H} . \end{aligned} \quad (49)$$

Due to the \mathbb{Z}_2 -symmetry about the $x = 0$ axis in Fig. 9, we denote the junction point I by $I(0, y_I)$. Since we send b to ∞ , the RT surface of $A \cup B \cup C$ will be very close to the horizon. Therefore, the sum of the total three geodesics is given by

$$2\tilde{D}((0, a, \epsilon), (0, 0, y_I)) + \tilde{D}((0, 0, y_H), (0, 0, y_I)) , \quad (50)$$

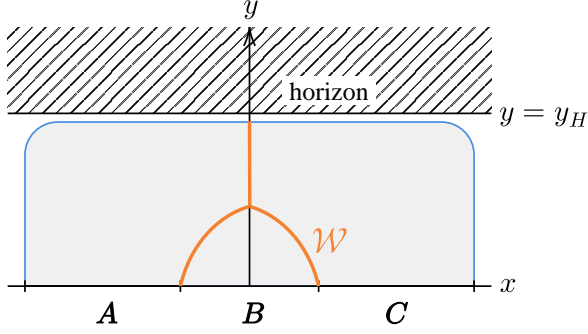


FIG. 9. The holographic dual of $S_R^{(q=3)}(A; B; C)$ at finite temperature.

with ϵ the UV cutoff. Minimizing (50) with respect to y_I , we end up with $y_I = \frac{\sqrt{3}y_H \sinh(a/y_H)}{2 \cosh(a/y_H) - 1}$ and

$$L[\mathcal{W}](a) = \operatorname{arccosh} \frac{2 \cosh \frac{a}{y_H} - 1}{\sqrt{3} \sinh \frac{a}{y_H}} + 2 \log \frac{2y_H \left(2 \cosh^2 \frac{a}{y_H} - |\cosh \frac{a}{y_H} - 2| - \cosh \frac{a}{y_H} \right)}{\sqrt{3}\epsilon \sinh \frac{a}{y_H}}. \quad (51)$$

Field-theoretical calculation.

From the CFT perspective, we need $\mathcal{Z}_{n^{q-1}, m}$, which can be obtained from the six-point function on a cylinder of infinite length and period β_{CFT}

$$\langle \sigma_1 \sigma_2 \sigma_3 \sigma_4 \sigma_5 \sigma_6 \rangle_{\text{cylinder}}, \quad (52)$$

with σ_i located at $\tau_i = 0$ and $x = x_i$, which is given by

$$\begin{aligned} x_6 &= -x_1 = b = \infty, \\ x_5 &= -x_2 = a + \epsilon, \\ x_4 &= -x_3 = a - \epsilon. \end{aligned} \quad (53)$$

The conformal weight of σ_i is given by (25) as before. To compute (52) we perform the conformal transformation (here $w_i = x_i + i\tau_i$)

$$z_i = 1 - \exp \frac{2\pi(w_2 - w_i)}{\beta_{\text{CFT}}}, \quad (54)$$

which sends $\{w_1, w_2, w_6\}$ to $\{\infty, 0, 1\}$ and $\{w_3, w_4, w_5\}$ to $\{z_3, z_4, z_5\}$. Following the same method as at zero temperature, we can numerically evaluate the derivative of the reflected multi-entropy with respect to a and compare it with the holographic result (51) as plotted in Fig. 10. Again these two results match precisely. The variation of reflected multi-entropy with respect to $y_H = \beta/(2\pi)$ for different interval length a is shown in Fig. 11. As the

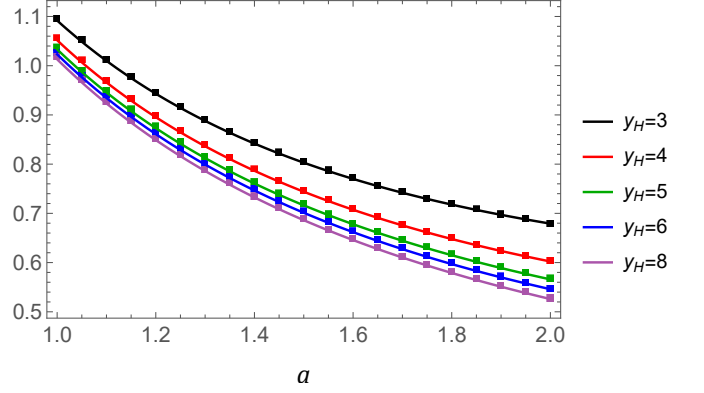


FIG. 10. The partial derivatives of $\frac{c}{3} L[\mathcal{W}]$ and $S_R^{(q=3)}$ (divided by $c/3$) with respect to a at different temperature are represented by lines and dots respectively.

temperature rises, the reflected multi-entropy decreases, which fits our expectations since in thermal CFT, the reflected entropy has similar behavior in the phase where the entanglement wedge cross section ends on the horizon (see Eq. (24) of [10] for example). As the parameter a (which characterizes the size of region B) increases, $S_R^{(3)}$ increases, indicating that it is a correlation measure for holographic states.

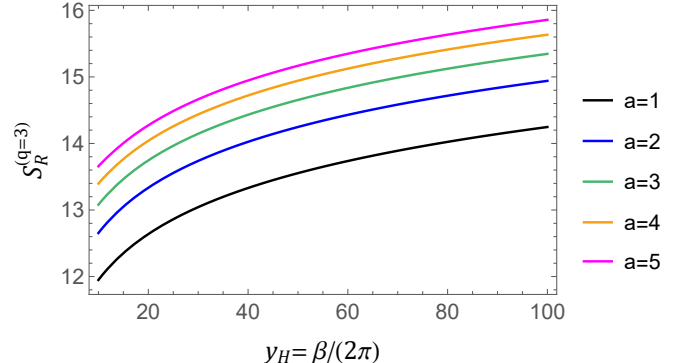


FIG. 11. The variation of reflected multi-entropy $S_R^{(q=3)}$ (divided by $c/3$) with respect to y_H for different a .

The OPE coefficient

The monodromy method can only determine the derivatives of the six-point function (45). To obtain the full field-theoretical results, we need to fix the OPE coefficients appearing in (37). There are two kinds of OPE coefficients, $c_{i,j}^a$ and $c_{a,b}^c$, with $i, j, \dots = 1, \dots, 6$ labeling the twist operators with conformal weights (25) and $a, b, c = 16, 23, 45$ labeling those with conformal weights (26). The OPE coefficient $c_{i,j}^a$ is similar to the OPE coefficient of reflected entropy, while $c_{a,b}^c$ is the

square of the OPE coefficient of multi-entropy. Let us first focus on $c_{i=2,j=3}^{a=23}$, which corresponds to the fusion $\sigma_2\sigma_3 \rightarrow \sigma_{23}$. We consider

$$\sigma_2 = \Sigma_A^{-1}, \quad \sigma_3 = \Sigma_B, \quad \sigma_{23} = \Sigma_A \Sigma_B^{-1}. \quad (55)$$

The three point function $\langle \sigma_2 \sigma_3 \sigma_{23} \rangle$ computes the partition function of the replica space, a mn^{q-1} -sheet Riemann surface, which in fact factorizes into n^{q-2} number of mn -sheet Riemann surfaces. The mn -sheet Riemann surface is nothing but the replica geometry appearing in the replica trick of reflected entropy (see appendix C of Ref. [13]), thus we have

$$\langle \sigma_2 \sigma_3 \sigma_{23} \rangle = \langle \sigma_{g_A^{-1}} \sigma_{g_B} \sigma_{g_A g_B^{-1}} \rangle^{n^{q-2}}, \quad (56)$$

where g_A and g_B are the twist operators for reflected entropy. Therefore, $c_{2,3}^{23}$ should be the n^{q-2} -th power of the reflected entropy OPE coefficient $C_{n,m}$,

$$\begin{aligned} c_{2,3}^{23} &= (C_{n,m})^{n^{q-2}} = (2m)^{-4h_{n,q}}, \\ \text{with } h_{n,q} &= \frac{c}{24} (n^{q-1} - n^{q-3}), \end{aligned} \quad (57)$$

which reduces to the OPE coefficient of reflected entropy when $q = 2$.

The other OPE coefficient, $c_{a=16,b=23}^{c=45}$, is the square of the multi-entropy OPE coefficient C_n (since in our case the corresponding conformal weights double), whose n -derivative can be fixed from holography [32, 34]

$$-\partial_n \log(c_{a,b}^c)|_{n=1} = -2\partial_n \log(C_n)|_{n=1} = c \log\left(\frac{2}{\sqrt{3}}\right). \quad (58)$$

With the result (57) and the assumption (58), the six-point function can be completely fixed as following: in the adjacent limit

$$|x_1 - x_6| = |x_2 - x_3| = |x_4 - x_5| = 2\epsilon \rightarrow 0, \quad (59)$$

the six-point function reduces to a three-point function

$$\begin{aligned} \langle \sigma_1 \sigma_2 \sigma_3 \sigma_4 \sigma_5 \sigma_6 \rangle &\rightarrow c_{1,6}^{16} c_{2,3}^{23} c_{4,5}^{45} \langle \sigma_{a=16} \sigma_{b=23} \sigma_{c=45} \rangle \\ &= (2m)^{-12h_{n,q=3}} \langle \sigma_a \sigma_b \sigma_c \rangle \end{aligned} \quad (60)$$

with $\sigma_{a=16}$ located at $x_a = (x_1 + x_6)/2$ and similar for σ_b, σ_c . The three-point function is given by

$$\langle \sigma_a \sigma_b \sigma_c \rangle = \frac{c_{a,b}^c}{(x_{ab}/(2\epsilon))^{2h_a+2h_b-2h_c} (x_{bc}/(2\epsilon))^{2h_b+2h_c-2h_a} (x_{ca}/(2\epsilon))^{2h_c+2h_a-2h_b}} = c_{a,b}^c \left[\frac{(2\epsilon)^3}{x_{ab} x_{bc} x_{ca}} \right]^{\frac{c}{6}(n^2-1)}, \quad (61)$$

where $x_{ab} \equiv |x_a - x_b|$ and we take the cutoff to be 2ϵ . With the adjacent limit result as an input, we can further use the monodromy method to determine the value of six-point function in all the parameter region (since the monodromy method determines the derivatives of the six-point function). The consistency between the field-theoretical and holographic results can also be verified in the adjacent limit. The field-theoretical result is given by

$$\begin{aligned} S_R^{(3)}[n] &= \frac{1}{1-n} \frac{1}{n} \log \langle \sigma_1 \sigma_2 \sigma_3 \sigma_4 \sigma_5 \sigma_6 \rangle \\ &= -12 \frac{1}{1-n} \frac{1}{n} h_{n,q=3} \log(2m) - \frac{c}{6} \frac{1}{1-n} \frac{1}{n} (n^2-1) \log \frac{x_{ab} x_{bc} x_{ca}}{(2\epsilon)^3} + \frac{1}{1-n} \frac{1}{n} \log c_{a,b}^c, \\ &= \frac{c}{6} \left(1 + \frac{1}{n}\right) \log \frac{x_{ab} x_{bc} x_{ca}}{m^3 \epsilon^3} + \frac{1}{1-n} \frac{1}{n} \log c_{a,b}^c. \end{aligned} \quad (62)$$

In the $m, n \rightarrow 1$ limit,

$$\begin{aligned} S_R^{(3)} &= \frac{c}{3} \log \frac{x_{ab} x_{bc} x_{ca}}{\epsilon^3} - \partial_n \log(c_{a,b}^c)|_{n=1} \\ &= \frac{c}{3} \log \frac{x_{ab} x_{bc} x_{ca}}{\epsilon^3} + c \log\left(\frac{2}{\sqrt{3}}\right), \end{aligned} \quad (63)$$

which is the same as $(c/3)L[\mathcal{W}]$ (see Ref. [34] for the calculation of $L[\mathcal{W}]$ in the adjacent limit).

* mkyuan19@fudan.edu.cn

† limy22@m.fudan.edu.cn

‡ yang_zhou@fudan.edu.cn

- [1] R. Horodecki, P. Horodecki, M. Horodecki, and K. Horodecki, Quantum entanglement, Rev. Mod. Phys. **81**, 865 (2009), arXiv:quant-ph/0702225.
- [2] L. Amico, R. Fazio, A. Osterloh, and V. Vedral, Entanglement in many-body systems, Rev. Mod. Phys. **80**, 517 (2008), arXiv:quant-ph/0703044.

- [3] J. M. Maldacena, The Large N limit of superconformal field theories and supergravity, *Adv. Theor. Math. Phys.* **2**, 231 (1998), arXiv:hep-th/9711200.
- [4] S. S. Gubser, I. R. Klebanov, and A. M. Polyakov, Gauge theory correlators from noncritical string theory, *Phys. Lett. B* **428**, 105 (1998), arXiv:hep-th/9802109.
- [5] E. Witten, Anti-de Sitter space and holography, *Adv. Theor. Math. Phys.* **2**, 253 (1998), arXiv:hep-th/9802150.
- [6] S. Ryu and T. Takayanagi, Holographic derivation of entanglement entropy from AdS/CFT, *Phys. Rev. Lett.* **96**, 181602 (2006), arXiv:hep-th/0603001.
- [7] S. Ryu and T. Takayanagi, Aspects of Holographic Entanglement Entropy, *JHEP* **08**, 045, arXiv:hep-th/0605073.
- [8] V. E. Hubeny, M. Rangamani, and T. Takayanagi, A Covariant holographic entanglement entropy proposal, *JHEP* **07**, 062, arXiv:0705.0016 [hep-th].
- [9] A. C. Wall, Maximin Surfaces, and the Strong Subadditivity of the Covariant Holographic Entanglement Entropy, *Class. Quant. Grav.* **31**, 225007 (2014), arXiv:1211.3494 [hep-th].
- [10] T. Takayanagi and K. Umemoto, Entanglement of purification through holographic duality, *Nature Phys.* **14**, 573 (2018), arXiv:1708.09393 [hep-th].
- [11] P. Nguyen, T. Devakul, M. G. Halbasch, M. P. Zaletel, and B. Swingle, Entanglement of purification: from spin chains to holography, *JHEP* **01**, 098, arXiv:1709.07424 [hep-th].
- [12] P. Caputa, M. Miyaji, T. Takayanagi, and K. Umemoto, Holographic Entanglement of Purification from Conformal Field Theories, *Phys. Rev. Lett.* **122**, 111601 (2019), arXiv:1812.05268 [hep-th].
- [13] S. Dutta and T. Faulkner, A canonical purification for the entanglement wedge cross-section, *JHEP* **03**, 178, arXiv:1905.00577 [hep-th].
- [14] H.-S. Jeong, K.-Y. Kim, and M. Nishida, Reflected Entropy and Entanglement Wedge Cross Section with the First Order Correction, *JHEP* **12**, 170, arXiv:1909.02806 [hep-th].
- [15] P. Hayden, O. Parrikar, and J. Sorce, The Markov gap for geometric reflected entropy, *JHEP* **10**, 047, arXiv:2107.00009 [hep-th].
- [16] J. Kudler-Flam and S. Ryu, Entanglement negativity and minimal entanglement wedge cross sections in holographic theories, *Phys. Rev. D* **99**, 106014 (2019), arXiv:1808.00446 [hep-th].
- [17] Y. Kusuki, J. Kudler-Flam, and S. Ryu, Derivation of holographic negativity in AdS_3/CFT_2 , *Phys. Rev. Lett.* **123**, 131603 (2019), arXiv:1907.07824 [hep-th].
- [18] X. Dong, X.-L. Qi, and M. Walter, Holographic entanglement negativity and replica symmetry breaking, *JHEP* **06**, 024, arXiv:2101.11029 [hep-th].
- [19] X. Dong, S. McBride, and W. W. Weng, Replica wormholes and holographic entanglement negativity, *JHEP* **06**, 094, arXiv:2110.11947 [hep-th].
- [20] X. Dong, J. Kudler-Flam, and P. Rath, Entanglement Negativity and Replica Symmetry Breaking in General Holographic States, (2024), arXiv:2409.13009 [hep-th].
- [21] K. Tamaoka, Entanglement Wedge Cross Section from the Dual Density Matrix, *Phys. Rev. Lett.* **122**, 141601 (2019), arXiv:1809.09109 [hep-th].
- [22] A. Mollabashi and K. Tamaoka, A Field Theory Study of Entanglement Wedge Cross Section: Odd Entropy, *JHEP* **08**, 078, arXiv:2004.04163 [hep-th].
- [23] M. Walter, D. Gross, and J. Eisert, Multi-partite entanglement, (2016), arXiv:1612.02437 [quant-ph].
- [24] S. Nezami and M. Walter, Multipartite Entanglement in Stabilizer Tensor Networks, *Phys. Rev. Lett.* **125**, 241602 (2020), arXiv:1608.02595 [quant-ph].
- [25] Y. Zou, K. Siva, T. Soejima, R. S. K. Mong, and M. P. Zaletel, Universal tripartite entanglement in one-dimensional many-body systems, *Phys. Rev. Lett.* **126**, 120501 (2021), arXiv:2011.11864 [quant-ph].
- [26] C. A. Agón, P. Bueno, O. Lasso Andino, and A. Vilari López, Aspects of N-partite information in conformal field theories, *JHEP* **03**, 246, arXiv:2209.14311 [hep-th].
- [27] G. Penington, M. Walter, and F. Witteveen, Fun with replicas: tripartitions in tensor networks and gravity, *JHEP* **05**, 008, arXiv:2211.16045 [hep-th].
- [28] V. E. Hubeny, M. Rangamani, and M. Rota, The holographic entropy arrangement, *Fortsch. Phys.* **67**, 1900011 (2019), arXiv:1812.08133 [hep-th].
- [29] T. He, M. Headrick, and V. E. Hubeny, Holographic Entropy Relations Repackaged, *JHEP* **10**, 118, arXiv:1905.06985 [hep-th].
- [30] S. Hernández-Cuenca, V. E. Hubeny, and H. F. Jia, Holographic entropy inequalities and multipartite entanglement, *JHEP* **08**, 238, arXiv:2309.06296 [hep-th].
- [31] A. Gadde, V. Krishna, and T. Sharma, New multipartite entanglement measure and its holographic dual, *Phys. Rev. D* **106**, 126001 (2022), arXiv:2206.09723 [hep-th].
- [32] A. Gadde, V. Krishna, and T. Sharma, Towards a classification of holographic multi-partite entanglement measures, *JHEP* **08**, 202, arXiv:2304.06082 [hep-th].
- [33] A. Gadde, S. Jain, V. Krishna, H. Kulkarni, and T. Sharma, Monotonicity conjecture for multi-party entanglement. Part I, *JHEP* **02**, 025, arXiv:2308.16247 [hep-th].
- [34] J. Harper, T. Takayanagi, and T. Tsuda, Multi-entropy at low Renyi index in 2d CFTs, *SciPost Phys.* **16**, 125 (2024), arXiv:2401.04236 [hep-th].
- [35] A. Gadde, S. Jain, and H. Kulkarni, Multi-partite entanglement monotones, (2024), arXiv:2406.17447 [quant-ph].
- [36] N. Bao and N. Cheng, Multipartite Reflected Entropy, *JHEP* **10**, 102, arXiv:1909.03154 [hep-th].
- [37] J. Chu, R. Qi, and Y. Zhou, Generalizations of Reflected Entropy and the Holographic Dual, *JHEP* **03**, 151, arXiv:1909.10456 [hep-th].
- [38] A related measure called the multipartite entanglement of purification has been investigated in [39, 40].
- [39] K. Umemoto and Y. Zhou, Entanglement of Purification for Multipartite States and its Holographic Dual, *JHEP* **10**, 152, arXiv:1805.02625 [hep-th].
- [40] N. Bao and I. F. Halpern, Conditional and Multipartite Entanglements of Purification and Holography, *Phys. Rev. D* **99**, 046010 (2019), arXiv:1805.00476 [hep-th].
- [41] In this Letter, we treat all the subsystems symmetrically.
- [42] Here we follow the definition in [34]. Compared with [31], we use a slightly different notation for the partition function on the replica space. We denote the partition function on the n^{q-1} -sheet Riemann surface by $\mathcal{Z}_{n^{q-1}}^{(q)}$ instead of $\mathcal{Z}_n^{(q)}$ in [31].
- [43] C. Holzhey, F. Larsen, and F. Wilczek, Geometric and renormalized entropy in conformal field theory, *Nucl. Phys. B* **424**, 443 (1994), arXiv:hep-th/9403108.
- [44] P. Calabrese and J. L. Cardy, Entanglement entropy

and quantum field theory, *J. Stat. Mech.* **0406**, P06002 (2004), arXiv:hep-th/0405152.

[45] P. Calabrese and J. Cardy, Entanglement entropy and conformal field theory, *J. Phys. A* **42**, 504005 (2009), arXiv:0905.4013 [cond-mat.stat-mech].

[46] The marriage with holographic purification was also mentioned in [32] without explicit construction.

[47] O. Lunin and S. D. Mathur, Correlation functions for $M^{**}N / S(N)$ orbifolds, *Commun. Math. Phys.* **219**, 399 (2001), arXiv:hep-th/0006196.

[48] See Supplemental Material for the derivation of the conformal weights for twist operators; the CFT computation of the twist operator six-point function; a discussion on the operator product expansion coefficients; and both the CFT computation and the holographic computation at finite temperature.

[49] For reflected entropy, we have [13]

$$h_{g_A} = h_{g_A^{-1}} = \frac{cn(m^2 - 1)}{24m},$$

where g_A and g_A^{-1} are the twist operators located at the two endpoints of interval A .

[50] The conformal dimension of the multi-entropy twist operator is given in Eq. (29) of [34].

[51] A. A. Belavin, A. M. Polyakov, and A. B. Zamolodchikov, Infinite Conformal Symmetry in Two-Dimensional Quantum Field Theory, *Nucl. Phys. B* **241**, 333 (1984).

[52] A. B. Zamolodchikov, Conformal symmetry in two-dimensional space: Recursion representation of conformal block, *Theor. Math. Phys.* **73**, 1088 (1987).

[53] T. Hartman, Entanglement Entropy at Large Central Charge, (2013), arXiv:1303.6955 [hep-th].

[54] M. Banados, C. Teitelboim, and J. Zanelli, The Black hole in three-dimensional space-time, *Phys. Rev. Lett.* **69**, 1849 (1992), arXiv:hep-th/9204099.

[55] T. D. Ellison and M. Cheng, Toward a Classification of Mixed-State Topological Orders in Two Dimensions, *PRX Quantum* **6**, 010315 (2025), arXiv:2405.02390 [cond-mat.str-el].

[56] Z. Wang, Z. Wu, and Z. Wang, Intrinsic Mixed-State Topological Order, *PRX Quantum* **6**, 010314 (2025), arXiv:2307.13758 [quant-ph].

[57] For tripartite case, [58] presents the following constraint

$$\frac{1}{m_{AB}} + \frac{1}{m_{BC}} + \frac{1}{m_{CA}} > 1, \quad m_{AB,BC,CA} \in \mathbb{Z}_+,$$

with m_{AB} the order of $\sigma_A^{-1}\sigma_B$. For the n -th Rényi multi-entropy ($m_{AB} = m_{BC} = m_{CA} = n$), this inequality is violated for $n > 2$, indicating replica symmetry breaking.

[58] A. Gadde, J. Harper, and V. Krishna, Multi-invariants and Bulk Replica Symmetry, (2024), arXiv:2411.00935 [hep-th].

[59] P. Hayden, M. Lemm, and J. Sorce, Reflected entropy: Not a correlation measure, *Phys. Rev. A* **107**, L050401 (2023), arXiv:2302.10208 [hep-th].

[60] P. Bueno and H. Casini, Reflected entropy for free scalars, *JHEP* **11**, 148, arXiv:2008.11373 [hep-th].

[61] The conformal weight of twist operator is given by [47]

$$h = \frac{c}{24} \sum_k p_k \left(k - \frac{1}{k} \right),$$

with p_k the number of k -cycles.

[62] This row contains nm replicas in total. For $n = 3$ and $m = 2$ case, this row corresponds to the green shaded part in Fig. 7.